

Multiport Converter for CubeSat

Muhaidheen M¹, Muralidharan S² and Vanaja N³

^{1,2,3}Department of EEE, Mepco Schlenk Engineering College, Sivakasi, India, muhai@mepcoeng.ac.in

*Correspondence: Muhaidheen M; Email: muhai@mepcoeng.ac.in;

ABSTRACT: Maximizing solar energy harvesting and miniaturizing DC-to-DC converters will be a difficult task for the CubeSat that operates in low earth orbit (LEO), where size and weight are limited. To maximize solar energy collection, the electrical power system (EPS) architectures use numerous separate DC-DC converters, which will be problem for miniaturization of whole model because several inductors will be used in each converter. The key purpose of this article is to demonstrate a topology of multiport converter that requires only one inductor and a small number of components, reducing the overall system size. The proposed system will have half-bridge modules with series connection, connected parallelly with PV panels will power the battery system through a DC-DC boost converter. On considering the 1U CubeSat standards a prototype is used to verify the performance of the proposed converter in numerous case scenarios.

General Terms: Power Converter, Energy Systems.

Keywords: Boost Converter, Converter topology, CubeSat, DC-DC Converter, Design Concept, Electric Power System, LEO Satellites, Multiple-input multiple-output (MIMO), Power Electronic Converters, Solar PV System, Switched Capacitor Converter (SCC).

ARTICLE INFORMATION

Author(s): Muhaidheen M, Muralidharan S and Vanaja N
 Received: 23/04/2022; Accepted: 22/06/2022; Published: 28/06/2022;
 E- ISSN: 2347-470X;
 Paper Id: IJEER220423;
 Citation: 10.37391/IJEER.100239
 Webpage-link:
<https://ijeer.forexjournal.co.in/archive/volume-10/ijeer-100239.html>



Publisher's Note: FOREX Publication stays neutral with regard to jurisdictional claims in Published maps and institutional affiliations.

1. INTRODUCTION

Due to the low manufacturing costs, faster manufacture, and ease of deployment, CUBESATS are the most common choice for space exploration these days. The CubeSats' EPS includes PV panels, lithium-ion batteries, power electronic converters for energy generation, energy storage and energy conversion respectively. The PV panels can be attached to the CubeSat's outer surfaces facing the Sun, or the panels can be a deployable one. Although deployable panels have the advantage of being able to be orientated towards the sun at any moment to generate maximum electricity, fixed panels will be used more frequently. The conventional CubeSat EPS design circuit is shown in Fig.2. The MPPT is a technique which is used in the cases of the variable power source to maximize energy extraction as per the requirement. As the conditions change, the efficiency of power transfer from the solar cell is affected by the amount of available sunlight, the temperature of the solar cells, and the electrical characteristics of the load, and those characteristics determine which characteristics give the highest power transfer.

1.1 Different types of converters

In the field of power electronics, there are four types of converters, in that the DC-DC converter is used for its efficient energy harvesting and consumption, as well as its storage behavior with minimal losses. The inputs and outputs of a DC-to-DC converter might be single or numerous. Based on the efficiency of each configuration, the DC-to-DC converters are further classified into 4 types, in that we recommend a Multiple-Input Multiple-Output (MIMO) converter. The MIMO converter allows users to have numerous inputs from diverse sources, and the combined input can be used on various loads which uses different output voltages profiles [10].

1.2 Different Stages of orbiting satellite

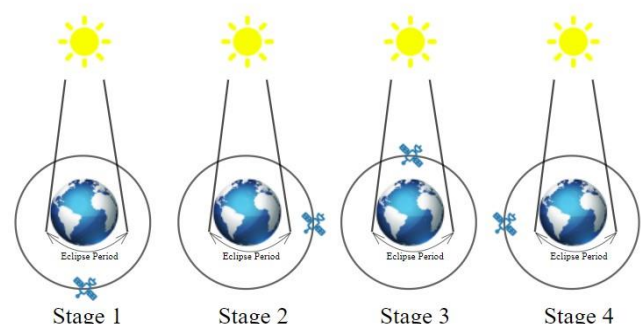


Figure 1: Stages of orbiting satellite

On considering a whole satellite in its orbit, it will function in four different stages as shown in figure 1. Assuming that initially the satellite is in eclipse region, in stage 1, during

eclipse period there will be no sunlight and so there will be no panel outputs and the rechargeable battery acts as the exclusive source for the satellite's payloads. In Stage 2, the satellite will start to get the irradiation from the Sun which leads to initial insolation period and the battery will be in charging state because during state 1 the battery will be in use and so it would get discharged. In stage 3, (assuming the satellite is in between the Sun and the Earth) the insolation period gets increased, and the yield output will be a maximum one. And eventually during the stage 4, the irradiation from the Sun starts decreasing because the satellite starts to go into eclipse period. This will be the satellite's one orbit cycle which gives 2 operational modes which are battery balanced mode and battery regulation mode [8].

1.3 Different types of Architectures

PV panels are positioned in opposing facets of CubeSat as shown in Fig. 2, which has a parallel connection because the CubeSat sides will receive solar irradiation irregularly. In the existing EPS topologies, each set of PV arrays use a DC-DC converter achieve MPPT operation despite significantly varying irradiation levels. During the day, the PV panels and the batteries will satisfy the demand depending on the payload's requirements. However, during the eclipse period, the battery meets the entire load demand. The battery is get charged or discharged according to the payload's demand is smaller or higher than the power generation.

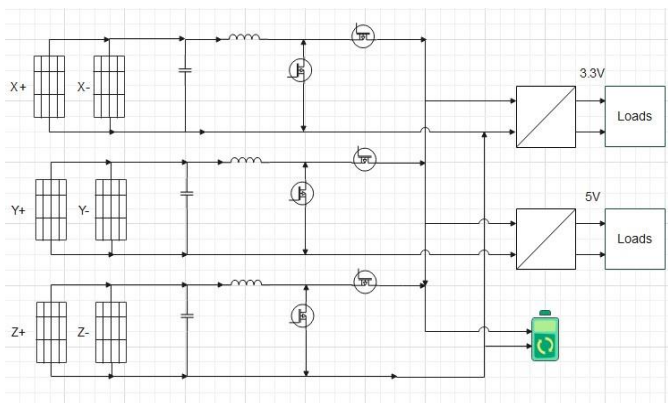


Figure 2: Conventional CubeSat EPS

For terrestrial PV systems to maximize energy harvest during mismatch situations such as partial shading, panel degradation, etc., Distributed MPPT (DMPPT) solutions will be the best option [11-15]. The DMPPT architectures are divided into two. They are differential power processor (DPP) architecture and full power processor (FPP) architecture. The conventional design has separate DC-to-DC converters for each PV modules in order to provide full MPPT under widely varying irradiation conditions. Whereas the DPP architecture exclusively uses the switching converters to handle the power divergence problem between the panels and the output from the series connection of the modules is handled by a central DC to DC converter. This not only decreases conversion loss, but it also shrinks the system's overall size and cost. There are two types of DPP architecture.

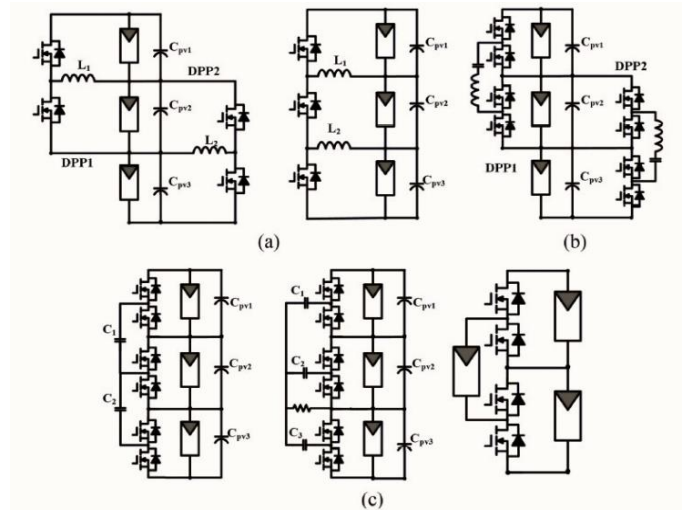


Figure 3: DPP (PV-to-PV) topologies (a) Switched Inductor (b) Resonant Switched Capacitor (c) Switched Capacitor Converters.

They are DPP in series and parallel connection. The typical CubeSat EPS, as seen in fig.2, is a parallel FPP which the uses several inductors. There are the three types of parallel-connected DPP architecture in that the PV-to-PV architecture is employed in our proposed system, and fig.3 shows the classification of converter topologies of PV-to-PV architecture. The goal of employing a single inductor in the DC-to-DC converter is attainable in this Switched Capacitor Converter (SCC) topology which provides a more compact solution. The SCC-based DPPs are further divided into three categories. They are direct configuration neighboring configuration and capacitorless configuration. When the SCC with a single inductor is used to run the PV modules under widely varying irradiation situations, there will some steep increase in conversion efficiency (maybe up to 80%). When compared to traditional LEO CubeSat EPS designs, the SCC-based DPP converter topology depicted in fig.3(c) results in a lower converter size since it eliminates the extra inductors and requires only one inductor [1]-[7] whereas, the other two configurations necessitate the use of more than one inductor of same rating in the EPS, constraining the compactness of the system. The true MPPT operation can't be achieved with this setup, even in terrestrial applications, and when considering CubeSat PV panels, which are further deteriorated with a higher percentage of irradiation levels divergence. And so, a new CubeSat converter design which accomplishes model miniaturization and solar energy harvest maximization will be useful.

2. PROPOSED WORK

The Fig.3 shows the proposed converter circuit, and the block diagram of our proposed work is shown in fig.4. In the fig.3 the PV module, a capacitor and a HB module are connected in parallel to employ the parallel DPP and IPS [4]-[7] architecture is employed as the DPP setup is connected in series with the other setups like this and the output of the whole module is sent to the central boost converter and to a battery. The whole operation of this setup is as follows. When the sun rays fall on the PV panels, the PV panel transfers

energy from the panel to the HB modules which are connected in such a way that they harvest the maximum energy from the PV panels and so the voltage is maintained at maximum power point voltage (v_{mpp}) and the current (i_{pv}) flows to the capacitors (C_{pv}) and from the capacitor (C_{pv}) turns into the inductor current (i_L) and transfers the energy to the battery system.

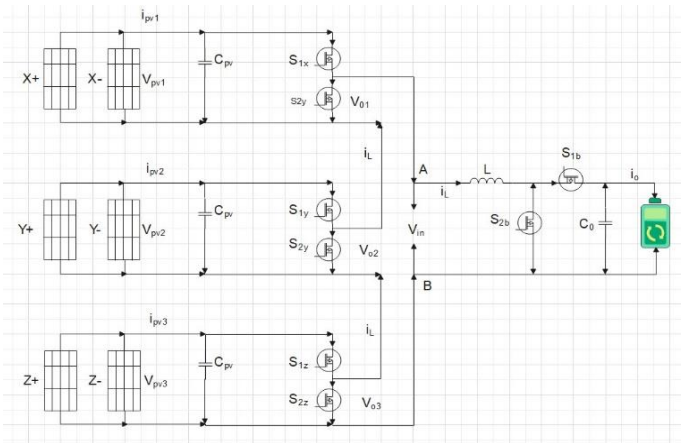


Figure 4: Proposed multiport converter circuit

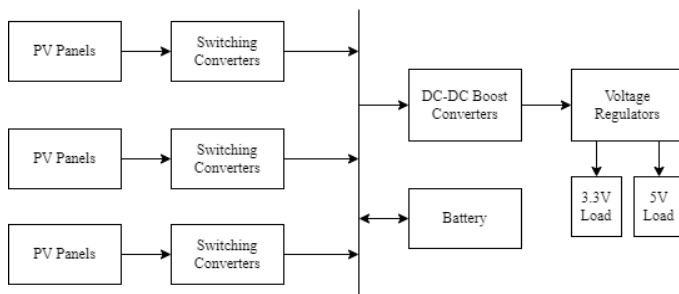


Figure 5: Block Diagram of Proposed Converter

The input of the boost converter is the output from the HB circuits, which is a multi-level stepped waveform. The HB module's operation is explained with the assumption that i_L is nearly a constant. Figure 5(a) and 5(b) depict the two modes of operation for a single HB module. Switches S1 and S2 work in complementary style that is when one switch is turned ON, the other switch will be in OFF state. The HB circuit enters insertion mode when switch S1 is turned on, in which a current of $i_L - i_{pv}$ flows out of the capacitor (C_{pv}) and the value of voltage across S2 (v_o) equals to the panel voltage (v_{pv}). The HB circuit enters bypass mode when switch S2 is turned on, in which the PV panel current (i_{pv}) flows directly into the capacitor (C_{pv}) and so the panel is separated from the circuit and so the output voltage (v_o) of the HB module when seen across S2 will be zero. The HB modules operation can be explained using the method depicted in fig.5. Operational modes of all HB modules altogether can be named as, mode0, mode1, mode2, mode3. These modes of operations are classified on the basis of ON state and OFF state of switches in half bridge (HB) modules as shown in fig.5. Each HB modules have a capacitor C_{pv} and 2 switches (say) upper and lower switches. On considering three HB modules in circuit, when all lower switches are turned ON, all switches will be in bypass mode and so the output will be equal to 0V which is

called mode 0. When one upper switch and the other lower switches are turned ON, upper switch will be in insertion mode and the other lower switches will be in bypass mode and so the output will be the voltage across a C_{pv} , and this is the mode 1. When two upper switches and one lower switch are turned ON, upper switches will be in insertion mode and lower switch will be in bypass mode and so the output will be an added-up voltage across two C_{pv} , and this is mode 2. When all the upper switches are turned ON, all switches will be in insertion mode and so the output will be an added-up voltage across all C_{pv} , and this is mode 3. The voltage across C_{pv} , will be equal to the voltage from the solar cells (v_{pv}). The Table I explains the output voltages during different modes of operation of HB modules when connected with a constant DC source of 5V considering three HB modules which is just for a study purpose because when using the solar cells, the voltage profiles from it will be completely different from a constant DC source.

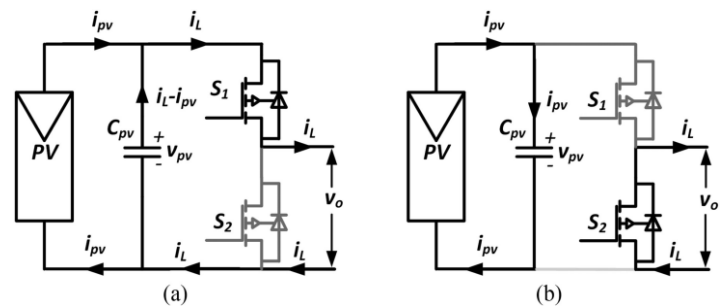


Figure 6: Single HB module's modes of operation

- (a) Insertion mode: S1 ON and S2 OFF
(b) Bypass mode: S1 OFF and S2 ON.

Table 1. OUTPUT VOLTAGES OF HB CIRCUITS

Operational modes	Output Voltage
Mode 0	0V
Mode 1	5V
Mode 2	10V
Mode 3	15V

3. CONVERTER DESIGN

When considering the various CubeSat operating situations, we chose the semiconductor switching frequencies as $f_s = 100$ kHz and the selection of other components are explained in the following sections.

4.1 Selection of I_{Lref}

The choice of I_{Lref} should ensure that MPPT monitoring is accurate and that conduction losses are kept to a minimum. For reliable MPPT monitoring, the value of $i_{Lref} = 0.55A$ should be larger than the currents from the PV panels and the rated MPP current (I_{mpp}) when operating at various irradiation levels.

$$I_{Lref} > i_{pv1}, i_{pv2}, i_{pv3}, I_{mpp}^r$$

4.1 Inductor Design

The inductor value for limiting the peak-to-peak ripple current (ΔI) in a conventional boost converter is computed as (resistive drops are neglected).

$$L \geq \frac{V_{in} \left(1 - \frac{V_{in}}{V_0} \right)}{\Delta I \times f}$$

The value of V_{in} in the suggested converter fluctuates because the PV panels' irradiation levels changes. When $V_{in} = 0.5 \times V_0$, the maximum value of L is necessary. As a result, the value of $L = 168.5 \mu\text{H}$ is obtained using the below equations,

$$L \geq \frac{0.25V_0}{\Delta I \times f}$$

4.1 Capacitor Design

As the HB module's operational modes are depicted in figure 5 (a) and (b), when S2 is turned on, it will be in the bypass mode, the PV panel capacitor C_{pv} charges with current I_{mppi} because the value of I_{mppi} varies according to the radiation circumstances, can also be substituted by I_{Lref} . When $D_i = 0.5$, the value of $C_{pv} = 330 \mu\text{F}$ can be derived using the below equations,

$$C_{pv} \frac{\Delta V_{pv}}{\Delta T} = I_{mppi}$$

$$C_{pv} \geq \frac{I_{Lref} D_i (1 - D_i)}{\Delta V \times f}$$

$$C_{pv} \geq \frac{0.25I_L}{\Delta V \times f}$$

The value of the capacitor in the converter side can also be calculated using those equations and so the value of capacitor $C = 900.9 \mu\text{F}$. Using the equations in section IV, the values of inductor and the capacitors in the HB module side and the converter side are calculated and tabulated as table II.

Table 2. SPECIFICATIONS OF COMPONENTS

Name	Values
Inductor	168.5 μH
Capacitor	330 μF and 900.9 μF
Switching Frequency	100 KHz

4 SIMULATION WORKS

The circuit that has been proposed is employed in MATLAB software and simulated to study the working of the circuit while considering several case studies. The MATLAB circuit model employing the proposed converter topology excited by constant DC source voltage of 5V as shown in figure 6 is simulated to obtain the output voltage of whole half bridge circuit as shown in the table 1 and the figure 7 shows multi-level stepped output waveform.

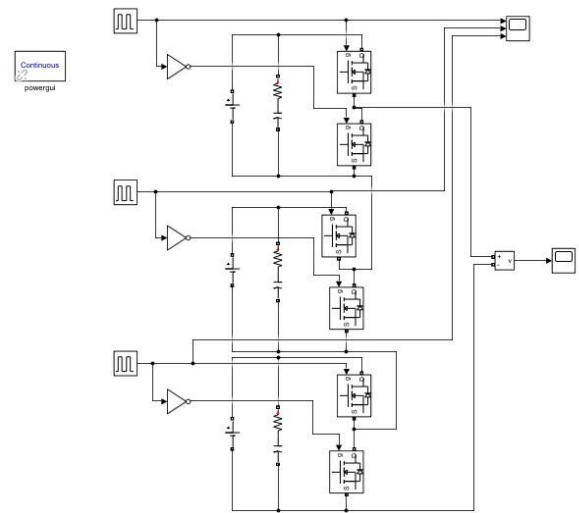


Figure 7: MATLAB half bridge circuit excited by DC sources

The DC sources are only being used for research purposes because the output voltages of PV panels will vary depending on the amount of sun that hits them, and the operating principles and control techniques are incompatible with CubeSat's EPS, which needs genuine MPPT functioning for all PV panels with significantly variable irradiance profiles. Figure 8 shows the proposed circuit (from MATLAB) which has the PV arrays as the sources connected to the HB circuit and to a battery via a boost converter and the output waveform of this MATLAB circuit model is displayed as the figure 9 which includes the inductor current profile, the load current and voltage profiles, and the battery profiles (right side of the figure 9).

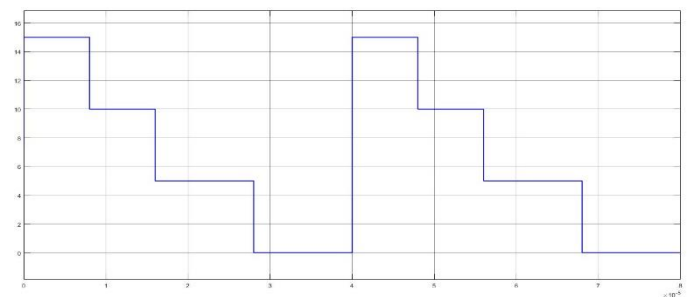


Figure 8: HB circuit's output waveform excited by DC sources

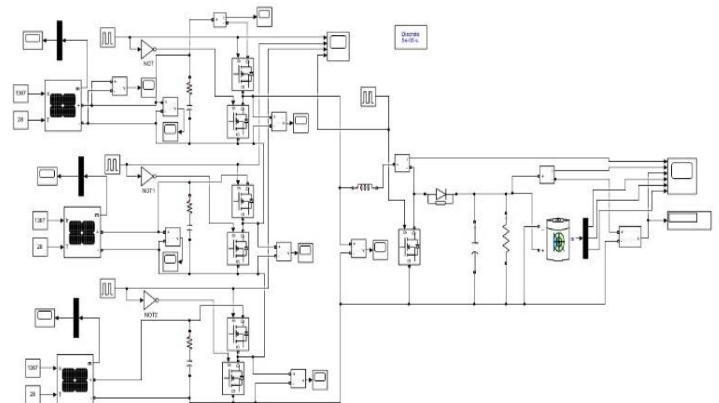


Figure 9: MATLAB circuit with PV array, Boost converter and PI inductor current control loop

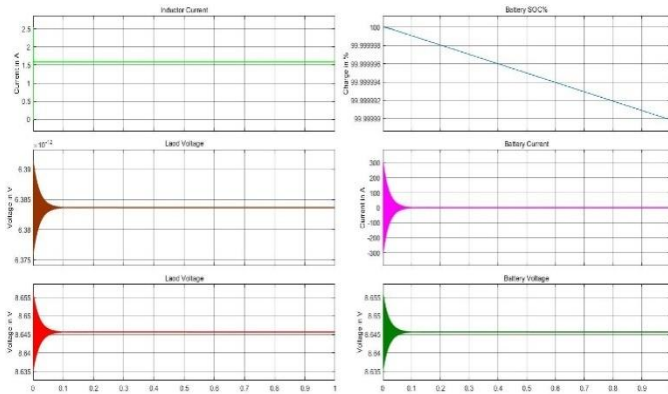


Figure 10: Output waveform of MATLAB circuit with PV array, Boost converter

4.1 Gate Signals

The Gate pulses given for the each MOSFET switches in the simulation has been shown in *fig.10* and the gate signal's duty cycle(last waveform in the *fig.10*) decides the output voltage and this is inferred from the below equation (considering standard boost converter),

$$V_0 = \frac{V_{in}}{1 - D}$$

In the *figure 10*, the duty cycles of the HB module switches are shown in the first three waveforms of the *figure 10* and the switches in each HB module undergo insertion mode and bypass mode complementarily as shown in the *fig.5* are the reasons for the stepped output waveform from the HB modules which will be the input for the boost converter.

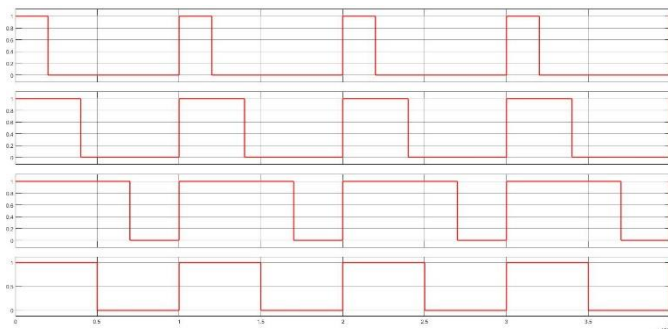
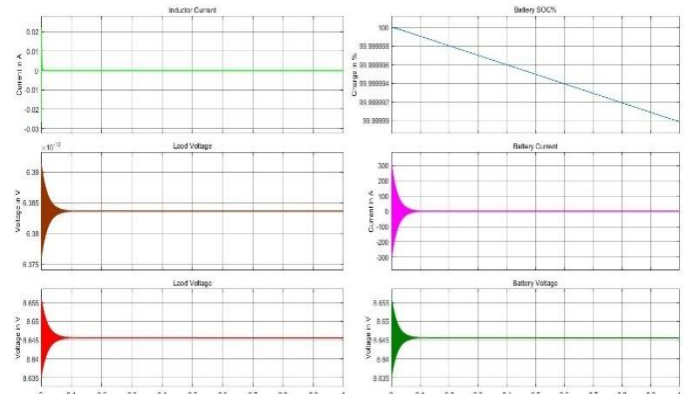


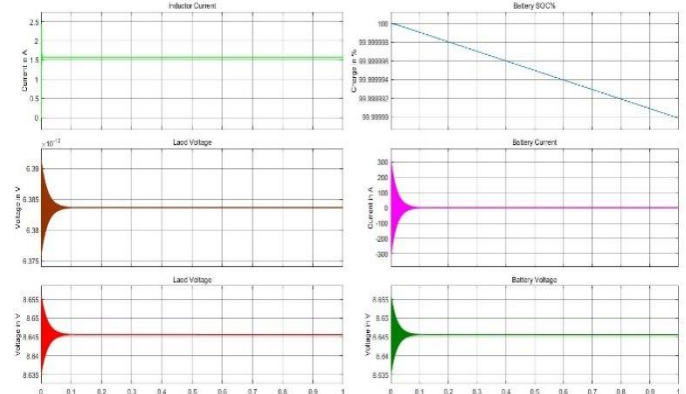
Figure 11: Gate Pulses of all switches

4.2 Case Studies

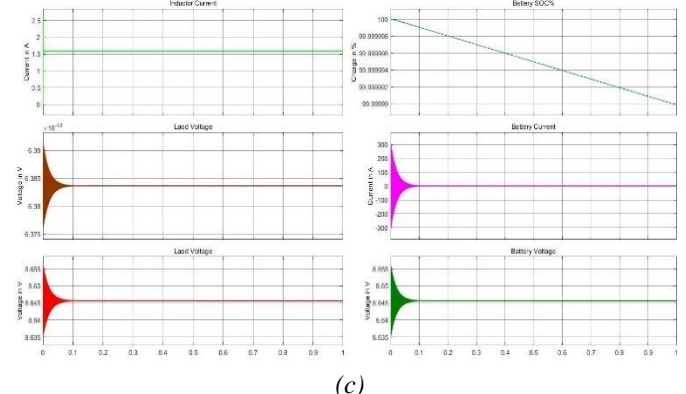
To know about the compensation of output voltage from the converter for powering the loads, some case studies are done. From the *fig.1*, when the satellite's PV panels receive no insolation, there will no output from the panels, but the battery will compensate the required output voltage and when the PV panel receives some insolation, there will be some output, but it is not enough for exciting the whole system and in this case, the battery will supply the required output voltage and when the PV panels get the maximum insolation, the whole system will get excited and the battery will be in the charging state because in the previous stages, the battery will get discharged while supplying the required output voltage.



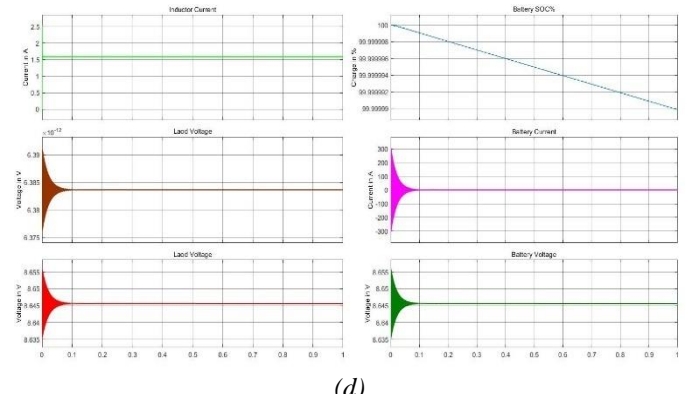
(a)



(b)



(c)



(d)

Figure 12: Case Studies (a) With 0 PV and Battery (b) With 1 PV and Battery (c) With 2 PV and Battery (d) With 3 PV and Battery

In the *fig.11*, it's seen that the inductor current changes when the number of PV panels that supply changes but the output voltage from the converter has no changes and in each picture the right shows the battery profile for each case.

5. DESIGN OF PROTOTYPE

On the basis of the 1U CubeSat (10cm*10cm*11cm) standards, a prototype is designed to study the converter's the performance, and a controller can also be designed. The Fig.10 shows the hardware prototype which has the components of specified values as shown in the table II and table III.

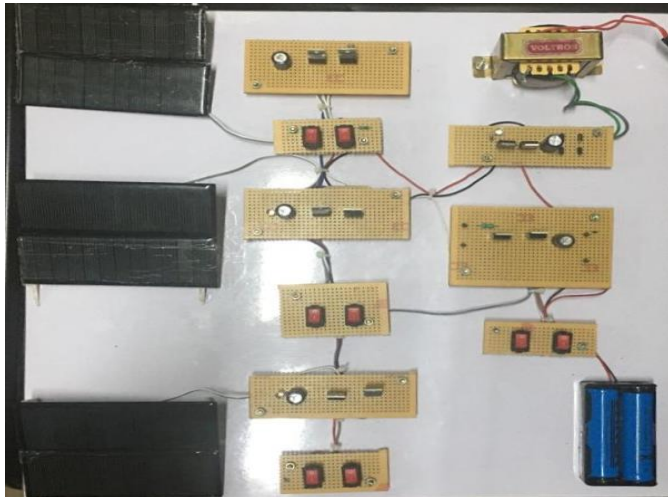


Figure 13: Hardware Prototype

Table 3. SPECIFICATIONS BASED ON 1 UNIT CUBESAT

Name	Specifications
PV Panel	$V_{oc}=5.38V$, $I_{sc} = 0.5196A$, $T = 28^{\circ}C$, $V_{mpp} = 4.818V$, $I_{mpp} = 0.5029A$, Irradiation = $1376W/m^2$ (considering the real-time scenarios)
Battery	2 Li-ion cells (in series) of 3.7V, 2200mAh
Switches	MOSFET IRF 540N

The Table 3 shows the key specifications based on 1U CubeSat. The equipment we used to study the prototype's behavior is DSO. Figure 11 shows the input voltage waveform of 3V DC taken from DSO which is given as input to the converter and the figure 12 shoes the output voltage waveform of 5V Dc taken from DSO which is the output from the whole system which also attains the required voltage profiles.

The power generation profile of PV panels in a conventional CubeSat is depicted in figure 13, where Pt signifies the total power generated by all PV panels. Throughout the eclipse, no power is generated because the entire system is powered by the battery, and total power generation ranges from $P_{pv,min} = 2.25W$ to $P_{pv,max} = 3.1W$ during the non-eclipse period. The CubeSats are meant to operate in an orbit with a height of 450kilometers above the sea level and with 51.6° of inclination angle and an orbital period of 96 mins long [11].

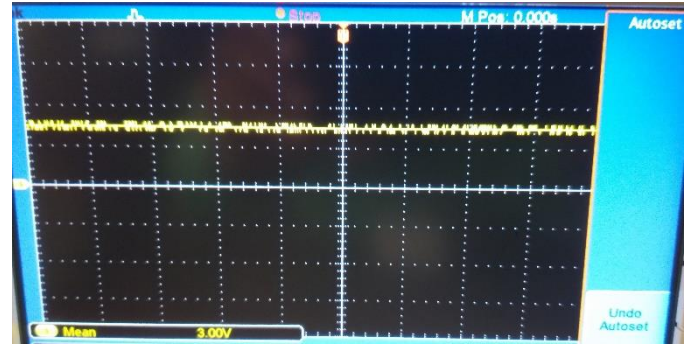


Figure 14: Input profile of Prototype

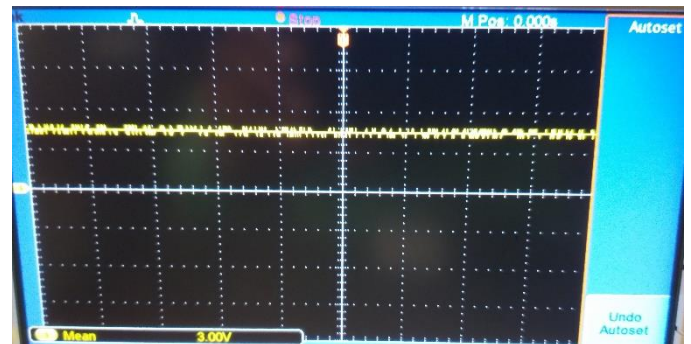


Figure 15: Output profile of Prototype

The power profile demonstrates that the PV panels work properly despite of any changes in the irradiation level at any time, the converter does not need to be built for total irradiation of PV panels' greatest power generating capabilities [11].

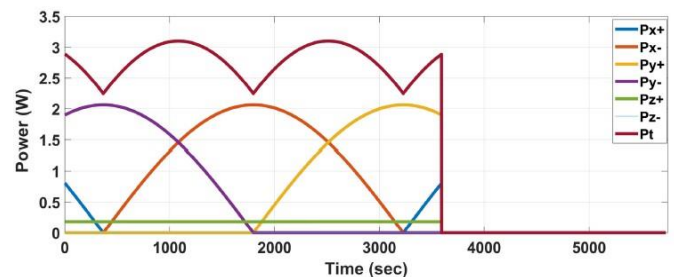


Figure 16: Power profile of PV panels in CubeSat when orbiting in the altitude of 450km

When compared to traditional EPS, the suggested converter requires four HB modules that is one more module will be used when compared to conventional type, but it requires only one inductor.

Table 4. Performance Comparison

Reference	Inductor	Switch	MPPT
[2]	n	2n	No
[3]	n	2n+2	No
Proposed	1	2n+2	yes

The gallium nitride field effect transistors with enhancement mode like LMG5200 integrated drivers can be used for HB modules. These devices were chosen because GaN devices run

at high frequencies can minimize the values of filter components and hence size get reduced and better controlling of converters can also be provide [9], but the IRF 540N was chosen because it is less expensive to produce the prototype. The output of half bridge circuit is fed to a boost converter (to boost up the solar output which can power the high voltage payloads) and to a battery storage system (to store energy which will be useful in time of no solar irradiation) and to 3.3V and 5V regulators to power the low voltage payloads. The dedicated PCB board and the controller can also be designed.

6. CONCLUSION

The Multiport converter we presented uses series-connected HB modules with PV inputs, with a boost converter connecting the output to battery terminals. As a consequence, the suggested converter harvests energy from PV panels with only one inductor. Each HB module may be set to maintain the voltage of the PV panel equal to the MPP voltage while keeping the inductor current within the restricted levels in the boost converter. To put the suggested principles to the test, a converter prototype employing the 1U CubeSat standards is developed and tested in a number of operational conditions. The results reveal that, despite being exposed to different irradiation circumstances, the suggested converter architecture performs as intended. Nonetheless, the suggested CubeSat EPS system is projected to work more consistently since it allows for redundant components, which are crucial for building and launching a CubeSat.

REFERENCES

- [1] B. Dobbs and P. Chapman, "A multiple-input DC-DC converter topology," *IEEE Power Electron. Lett.* vol. 1, no. 1, pp.6-9, 2003.
- [2] H. Behjati and A. Davoudi, "A multiple-input multiple-output DC-DC converter," *IEEE Trans. Ind. Appl.*, vol. 49, no. 3, pp. 1464–1479, May/June 2013.
- [3] Y. Jiang, J. A. A. Qahouq, M. Orabi, and M. Youssef, "PV solar system with multiple input power converter operating in discontinuous conduction mode and MPPT control," in *Proc. 35th Int. Telecomm. Ener. Conf. Smart Power EFF.*, 2013, pp. 1–5.
- [4] X. L. Li, Z. Dong, C. K. Tse, and D. D.-C. Lu, "Single-inductor multi-input multi-output DC-DC converter with high flexibility and simple control," *IEEE Trans. Power Electron.*, vol. 35, no. 12, pp. 13104–13114, Dec. 2020.
- [5] A. H. Chander and L. Kumar, "Multiple input converter for Standalone photovoltaic applications," in *Proc. 14th IEEE India Council Int. Conf.*, 2017, pp. 1–6.
- [6] R. Ahmadi and M. Ferdowsi, "Double-input converters based on h-bridge cells: Derivation, small-signal modeling, and power sharing analysis," *IEEE Trans. Circuits Syst. I*, vol. 59, no. 4, pp. 875–888, Apr. 2012.
- [7] Y. Li, X. Ruan, D. Yang, F. Liu, and C. K. Tse, "Synthesis of multiple input DC/DC converters," *IEEE Trans. Power Electron.*, vol. 25, no. 9, pp. 2372–2385, Sep. 2010.
- [8] Z. Qian, O. Abdel-Rahman, H. Al-Atrash, and I. Batarseh, "Modeling and Control of Three-Port DC/DC converter interface for satellite applications," *IEEE Trans. Power Electron.*, vol. 25, no. 3, pp. 1374–1765, March 2010.
- [9] M. Shah, A. Juneja, S. Bhattacharya, and A.G. Dean, "High frequency GaN device-enabled CubeSat EPS with real-time scheduling," *IEEE Energy Conversion Congress and Exposition (ECCE)*, pp. 2934–2941, Sep. 2012.
- [10] F. Ahmad, A.A. Haider, H. Naveed, A. Mustafa, and I. Ahmad, "Multiple Input Multiple Output DC to DC Converter," *5th International Multi-Topic ICT Conference (IMTIC)*, April 2018.
- [11] A. Edpuganti, V. Khadkikar, M. S. El Moursi, H. Zeineldin, "A Novel Multiport converter interface for solar panels of CubeSat," *IEEE Trans. Power Electron.*, vol. 37, no. 1, Jan. 2022.
- [12] Dr. S. Muralidharan, Dr. J. Gnanavadeivel, Dr. M. Muhaidheen and Dr. Menaka, "Harmonic Elimination In Multilevel Inverter Using Tlbo Algorithm For Marine Propulsion System", *Marine Technology Society Journal*, Volume No: 55, Issue No: 2; Page No: 117-126. DOI: 0.4031/MTSJ.55.2.13;
- [13] Sachin B. Shahapure, Vandana A. Kulkarni (Deodhar) and Sanjay M. Shinde, "A Technology Review of Energy Storage Systems, Battery Charging Methods and Market Analysis of EV Based on Electric Drives", *International Journal of Electrical and Electronics Research (IJEER)*, Volume 10, Issue 1 , Pages : 23-35 . March 2022.
- [14] M Rupesh and Dr. T S Vishwanath, "Fuzzy and ANFIS Controllers to Improve the Power Quality of Grid Connected PV System with Cascaded Multilevel Inverter", *International Journal of Electrical and Electronics Research (IJEER)*, volume 9, Issue 4, Pages: 89-95, Jan 2022.
- [15] Femy P. H., Jayakumar J, A Review on the Feasibility of Deployment of Renewable Energy Sources for Electric Vehicles under Smart Grid Environment", *International Journal of Electrical and Electronics Research (IJEER)*, Volume 9, Issue 3, Pages: 57-65, January 2022.



© 2022 by Muhaidheen M, Muralidharan S and Vanaja N. Submitted for possible open access publication under the terms and conditions of the Creative Commons Attribution (CC BY) license (<http://creativecommons.org/licenses/by/4.0/>).